

Pressure-induced Development of Dislocations at Elastic Discontinuities

By G. DAS† and S. V. RADCLIFFE

Department of Metallurgy and Materials Science,
Case Western Reserve University, Cleveland, Ohio

[Received 4 October 1968 and in final form 29 April 1969]

ABSTRACT

The stress fields around spherical elastic discontinuities in an isotropic solid subjected to externally applied hydrostatic pressure have been computed on the basis of a continuum mechanics model. The results have been compared with transmission electron microscopy observations of the pressure-induced development of dislocations in tungsten containing particles (thoria and hafnium carbide) or internal voids and in a model system of copper containing helium bubbles with the principal objective of elucidating the factors controlling the formation of such dislocations.

For the tungsten, no new dislocations were developed up to 25 kilobars, but they were observed at ThO_2 and HfC particles following pressurization to some 40 kilobars. The computed value of the maximum induced shear stress at that pressure is much below that required for dislocation nucleation. These observations of pressure-induced dislocations are interpreted in terms of additional stress concentrations associated with surface irregularities at the particles. In contrast to the tungsten, pressure-induced dislocations were observed around the helium bubbles in copper for a pressure (25 kilobars) in keeping with that predicted from the model.

For both the tungsten and the copper systems, the development of pressure-induced dislocations depends strongly on the size of the elastic discontinuities. This result is shown to be in keeping with the interpretation of the mechanism of the development of pressure-induced dislocations as one of nucleation rather than multiplication of pre-existing dislocations.

§ 1. INTRODUCTION

For several polycrystalline metals containing localized elastic discontinuities—iron containing particles of Fe_3C and FeO (Radcliffe and Warlimont 1964), chromium containing Cr_2O (Garrod and Wain 1965) and beryllium containing iron beryllide (Andrews and Radcliffe 1967)—the development of dislocations at the discontinuities as the result of the application of external hydrostatic pressure has been demonstrated from transmission electron microscopy observations. Since the introduction of fresh dislocations in this way at room temperature, as reviewed recently (Radcliffe 1969), can lead to marked changes in the mechanical behaviour of certain metals, it is important to develop a quantitative understanding of the mechanism by which such dislocations are formed.

† Now at International Business Machines Corporation, Components Division, East Fishkill, New York.

The hypothesis (Radcliffe 1964, Bullen, Henderson, Hutchison and Wain 1964) that generation of dislocation occurs as the result of localized shear stresses developed from differential elastic compression of the matrix and particle is qualitatively in keeping with the prismatic dislocation arrays that have been observed. Approximate values of the shear stresses induced in this way were computed, on the basis of a general solution obtained by Edwards (1951) for the stress distribution around a spheroidal inclusion in an arbitrary uniform state of stress, by Hahn and Rosenfield (1966) in a comparison of the effects of differential strains developed by particle growth, thermal contraction on cooling and external hydrostatic pressure. A general analysis (using a sequence of imaginary cutting, straining and welding operations) for the determination of the elastic field of an ellipsoidal inclusion and the way in which the presence of an inclusion having elastic constants different from those of the rest of the material disturbs an applied stress-field was developed by Eshelby (1957). However, this approach was not applied specifically to analyse the stresses developed under externally applied hydrostatic pressure at the interface of the inclusion and matrix for the general case where both have finite but different compressibilities. A particular difficulty in developing quantitative models is that for the systems in which pressure-induced dislocations have been observed previously the relevant elastic constants for the second phases are unknown or not well established.

The present investigation was undertaken with the principal objectives of calculating the stresses at the interface of an elastic particle in an isotropic matrix upon subjection of the system to high hydrostatic pressure in order to define the conditions for dislocation generation and of comparing the calculated conditions with those observed experimentally in the following systems: (a) tungsten—as an isotropic matrix—containing voids or different types of solid particles (ThO_2 and HfC) of second phase, and (b) a model system in which the elastic properties of the matrix and second phase are known and the matrix has a low flow stress. For the latter system, copper containing internal voids was selected. Transmission electron microscopy was used to examine the effects of pressurization up to 40 kilobars on the dislocation structure adjacent to the elastic discontinuities in these various systems.

§ 2. ELASTIC STRESS DISTRIBUTION AROUND A SPHERICAL INCLUSION IN AN ISOTROPIC SOLID UNDER HYDROSTATIC STRESS

A local elastic discontinuity in an isotropic solid represents a discrete region where the elastic properties are different from those in the matrix. Voids and rigid inclusions are the limiting cases where the values of the bulk moduli of the discontinuity are zero and infinity respectively. The presence of such discontinuities perturbs an otherwise uniform stress in a solid; for example, Goodier (1933) calculated that the stress-concentration increased by a factor of approximately 3 near a spherical cavity in an isotropic solid subjected to uniform tension.

While the general solution of the elastic stress field around a cavity in an isotropic matrix subjected to high hydrostatic pressure has been known since the classical work of Lamé in 1852, the extension of these calculations to the case of an elastic inclusion taking into specific consideration of the differences in compressibilities between matrix and inclusion has not been reported. The calculations made here† follow the continuum mechanics principles outlined by Sokolnikoff (1956) and assume that the elastic properties of the matrix and the inclusion are isotropic, the inclusion is spherical with a smooth surface and the stress fields of different particles do not interact. Under these conditions, the maximum shear stress, τ_{\max} , which develops at the inclusion-matrix interface is given by the following relationships for the cases of a cavity, cavity with internal pressure, a rigid inclusion and an elastic inclusion:

Cavity: $\tau_{\max} = \frac{3}{4}P$ (1)

Cavity with internal pressure P_i and external pressure zero: $\tau_{\max} = \frac{3}{4}P_i$ (2 a)

Cavity with internal pressure P_i and external pressure P : $\tau_{\max} = \frac{3}{4}(P - P_i)$ (2 b)

Rigid inclusion: $\tau_{\max} = \frac{G}{K} \cdot P$ (3)

Elastic inclusion: $\tau_{\max} = \frac{3G}{K} \left[\frac{K - K_i}{3K_i + 4G} \right] \cdot P$ (4)

where G is the shear modulus of the matrix, P is the applied hydrostatic pressure, P_i the internal pressure in the cavity and K and K_i are the bulk moduli of the matrix and the inclusion respectively. On substituting values of K_i appropriate to the limiting cases of the cavity and the rigid inclusion (i.e. zero and infinity), eqn. (4) reduces to eqns. (1) and (3) respectively.

The complete set of equations for the radial, circumferential and maximum shear stresses are given in table 1 for the cases of a cavity, rigid inclusion and elastic inclusion (the corresponding strains and other details of the calculations can be obtained from the authors). The table also contains the value of τ_{\max} for inclusions as calculated by Hahn and Rosenfield‡ (1966). Table 2 gives the values of the maximum shear stress computed from the equation in table 1 as a function of the externally

† An alternative approach to that used here for the elastic particle is the generalized misfit-strain type of analysis developed by Eshelby (1957) subsequent to the work of Nabarro (1940). As is discussed later, Lally and Partridge (1966) have used an extension of Eshelby's approach in an attempt to compute matrix shear stresses adjacent to a cavity containing gas at high pressure.

‡ While their approximation is useful for the case of the inclusion, it is inapplicable to the limiting case of an internal cavity. See table 1.

Hutchison and
 sult of localized
 pression of the
 ismastic disloca-
 es of the shear
 is of a general
 ution around a
 s, by Hahn and
 erential strains
 ng and external
 ce of imaginary
 mination of the
 ch the presence
 ose of the rest
 ped by Eshelby
 ally to analyse
 tic pressure at
 ase where both
 r difficulty in
 hich pressure-
 relevant elastic
 established.
 cipal objectives
 particle in an
 ostatic pressure
 n and of com-
 experimentally
 ix—containing
 f second phase,
 of the matrix
 ow stress. For
 lected. Trans-
 the effects of
 are adjacent to

INCLUSION IN PRESS

sents a discrete
 in the matrix.
 e values of the
 ectively. The
 iform stress in
 ress-concentra-
 cal cavity in an

Table 1. Calculated values of radial, circumferential and shear stresses developed in the matrix for the cases of cavity, rigid and elastic inclusion upon subjection to external hydrostatic pressure

Case	Reference	σ_{rr} in matrix	$\sigma_{\theta\theta}$ in matrix ($=\sigma_{\phi\phi}$)	Absolute value of τ_{\max} (at $r=a$) in matrix
I. Cavity (a) Zero internal pressure	Present calculation	$-P(1-a^3/r^3)$	$-P[1+1/2(a/r)^3]$	$3/4 P$
	Present calculation	$-P_1(a/r)^3$	$P_1/2(a/r)^3$	$3/4 P_1$
	Present calculation	$-P+(P-P_1)\frac{a^3}{r^3}$	$-P-(P-P_1)\frac{a^3}{2r^3}$	$3/4 (P-P_1)$
II. Rigid inclusion	Hahn and Rosenfield's (1966) equation	—	—	$\approx P/3$
	Present calculation	$-P \left[1 + \frac{2(1-2\nu)}{1+\nu} \cdot (a/r)^3 \right]$	$-P \left[1 - \frac{1-2\nu}{1+\nu} \cdot (a/r)^3 \right]$	$(G/K) \cdot P$
III. Elastic inclusion	Hahn and Rosenfield (1966)	—	—	$(P/3) \left[\frac{(K-K_i)}{K_i} \right]^\dagger$
	Present calculation	$-P \frac{3E_i(1-\nu)}{(1+\nu)E_i+2(1-2\nu_i)E}$ at $r=a$	$-P \frac{3\nu E_i+3(1-2\nu_i)E}{(1+\nu)E_i+2(1-2\nu_i)E}$ at $r=a$	$\frac{3PG}{K} \left[\frac{K-K_i}{3K_i+4G} \right]$

† Note: τ_{\max} in Hahn and Rosenfield's equation goes to infinity as $K_i \rightarrow 0$.

$-P$: External hydrostatic pressure,
 ν, ν_i : Poisson's ratio of the matrix
 and inclusion, respectively,
 K, K_i : Bulk modulus of the matrix
 and inclusion, respectively,

$(-P_i)$: Internal pressure,
 r : Radius vector,
 τ_{\max} : Maximum shear stress,
 $\sigma_{rr}, \sigma_{\theta\theta}, \sigma_{\phi\phi}$: Radial, circumferential and
 azimuthal stress, respectively,

a : The radius of the inclusion,
 G : Shear modulus of the matrix,
 E, E_i : Young's modulus of the matrix
 and inclusion, respectively.

Table 2. Calculated stress τ_{\max} at spherical cavity, rigid and elastic inclusion, in copper matrix as a function of the applied hydrostatic pressure

τ_{\max} (p.s.i.)	Elastic inclusion†

	Present calculation	$(1+\nu)E_1+2(1-2\nu)E$ at $r=a$	$(1+\nu)E_1+2(1-2\nu)E$ at $r=a$	$K \sqrt{3K_1+4G}$
--	---------------------	-------------------------------------	-------------------------------------	--------------------

† Note: τ_{\max} in Hahn and Rosenfeld's equation goes to infinity as $K_1 \rightarrow 0$.

$-P$: External hydrostatic pressure,
 ν, ν_1 : Poisson's ratio of the matrix
and inclusion, respectively,
 K, K_1 : Bulk modulus of the matrix
and inclusion, respectively,

$(-P_1)$: Internal pressure,
 r : Radius vector,
 τ_{\max} : Maximum shear stress,
 $\sigma_{rr}, \sigma_{\theta\theta}, \sigma_{\phi\phi}$: Radial, circumferential and
azimuthal stress, respectively,

a : The radius of the inclusion,
 G : Shear modulus of the matrix,
 E, E_1 : Young's modulus of the matrix
and inclusion, respectively.

and copper matrix as a function of the applied hydrostatic pressure

Matrix	Hydrostatic pressure	τ_{\max} (p.s.i.)									
		Cavity				Rigid inclusion	Elastic inclusion†				
		With zero internal pressure		With internal pressure (helium bubble)†			Thorium dioxide		Hafnium carbide		
Tungsten	10 kb	111×10^3	$\frac{G}{200}$	—	—	79×10^3	$\frac{G}{275}$	24.7×10^3	$\frac{G}{900}$	17.0×10^3	$\frac{G}{1300}$
	20 kb	222×10^3	$\frac{G}{100}$	—	—	159×10^3	$\frac{G}{137.5}$	49.4×10^3	$\frac{G}{450}$	34.0×10^3	$\frac{G}{650}$
	25 kb	278×10^3	$\frac{G}{80}$	—	—	200×10^3	$\frac{G}{110}$	61.8×10^3	$\frac{G}{360}$	42.5×10^3	$\frac{G}{520}$
	40 kb	444×10^3	$\frac{G}{50}$	—	—	318×10^3	$\frac{G}{68.8}$	98.8×10^3	$\frac{G}{225}$	68.0×10^3	$\frac{G}{325}$
Copper	10 kb	111×10^3	$\frac{G}{60}$	98×10^3	$\frac{G}{68}$	61×10^3	$\frac{G}{108}$	—	—	—	—
	20 kb	222×10^3	$\frac{G}{30}$	196×10^3	$\frac{G}{34}$	122×10^3	$\frac{G}{54}$	—	—	—	—
	25 kb	278×10^3	$\frac{G}{24}$	245×10^3	$\frac{G}{27}$	153×10^3	$\frac{G}{43.5}$	—	—	—	—

Data† used in the stress calculations for tungsten and copper.

	Tungsten	Thorium dioxide	Hafnium carbide	Copper
Shear modulus G (p.s.i.)	22×10^6	—	—	6.6×10^6
Young's modulus E (p.s.i.)	56.5×10^6	—	—	16.1×10^6
Poisson's ratio ν	0.27	—	—	0.33
Bulk modulus K (p.s.i.)	40.9×10^6	25.9×10^6	30.7×10^6	15.8×10^6

† Calculated on the basis of an internal pressure of 1.2 kb for the size of the bubble of 500 Å in radius.

‡ All data taken from Cottrell (1964 b) except for ThO_2 and HfC (Shaffer 1964).

applied hydrostatic pressure for cavities and thoria and hafnium carbide particles in a tungsten matrix and for helium bubbles in a copper matrix. It is seen that the induced stresses in the tungsten matrix, even at 25 kilobars, are substantially less than $G/30$, the stress theoretically required to create dislocations in a perfect crystal (Cottrell 1964 a). However, for copper containing helium bubbles the value of the maximum shear stress developed at the matrix-cavity interface at 25 kilobars exceeds the stress for dislocation nucleation.

§ 3. MATERIALS AND EXPERIMENTAL PROCEDURES

The details of the formation of internal voids in powder metallurgy (PM) tungsten have been published elsewhere (Das and Radcliffe 1968 a). In the present case, voids were developed in PM doped tungsten wire (0.030 in. in diameter) by annealing in vacuum at 2200°C for 30 min. The voids, which formed in stringers parallel to the axis of the wire, were generally spherical in shape and ranged in size from a few hundred up to 1000 Å. A tungsten-thoria alloy containing 0.9 vol. % ThO₂ was obtained in the form of rod (0.125 in. diameter) in the as-worked condition. Transverse sections (0.02 in. thick) were cut from the rod by spark-discharge machining. These disc specimens were annealed in vacuum at 2200°C for 30 min in order to develop isolated, rounded thoria particles free from dislocations. A tungsten-hafnium carbide alloy containing 1.4 vol. % HfC was obtained in the form of 0.025 in. thick sheet prepared from electron-beam melted material and solution treated and cooled so as to precipitate the carbide as fine particles. For the model system (i.e. copper containing helium bubbles), high purity polycrystalline copper (99.999% Cu) in the form of annealed sheet (0.025 in. thick), prepared by rolling a zone-refined single crystal, was irradiated with 43 mev alpha-particles in the cyclotron at Argonne National Laboratory to a total dose of 1.4×10^{17} particles cm⁻². On subsequent annealing at 750°C for one hour, helium bubbles were precipitated. These particular annealing conditions were selected to develop large bubbles, on the basis of previous studies of helium precipitation in copper (Barnes, Redding and Cottrell 1958, Barnes and Mazey 1960, Ghosh, Beevers and Barnes 1960). Pressurizing up to 25 kilobars at room temperature was carried out on specimens of these various systems in a modified piston-cylinder apparatus of the Bridgman-Birch type. An equi-volume mixture of n-pentane and isopentane was used as the pressure fluid and the pressure was measured from the change in electrical resistance of a manganin wire gauge within the pressure chamber. For higher pressures, a stainless steel capsule filled with the fluid was used in a MIA-1 (hybrid, belt or conical type) apparatus (Tanner and Radcliffe 1962).

Thin foils for electron microscopy were prepared by a combination of high precision microjet dimpling and final bath polishing (Das and Radcliffe 1968 b) from the wire samples of tungsten, the rod and sheet

specimens of tungsten alloys and from thin strips (0.125 in. \times 0.02 in. \times 0.010 in.) of the copper spark-cut to give a transverse section of the helium-rich layer.

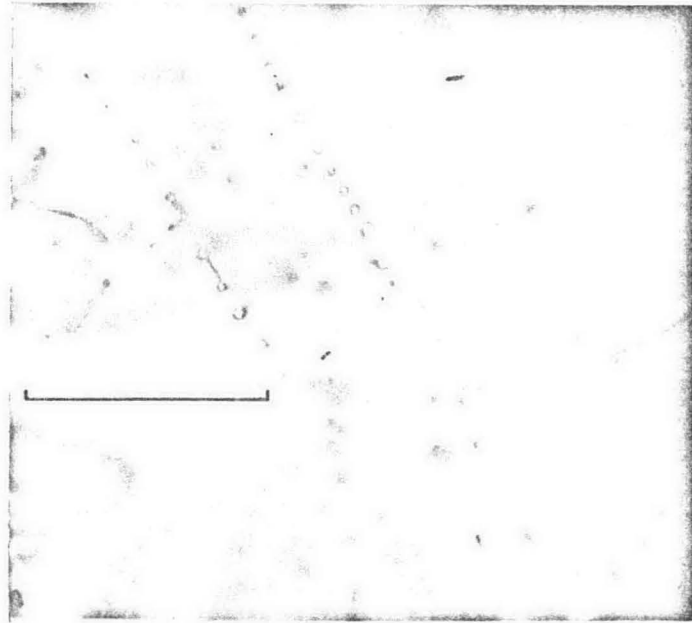
§ 4. RESULTS AND DISCUSSION

4.1. Tungsten and Tungsten Alloys

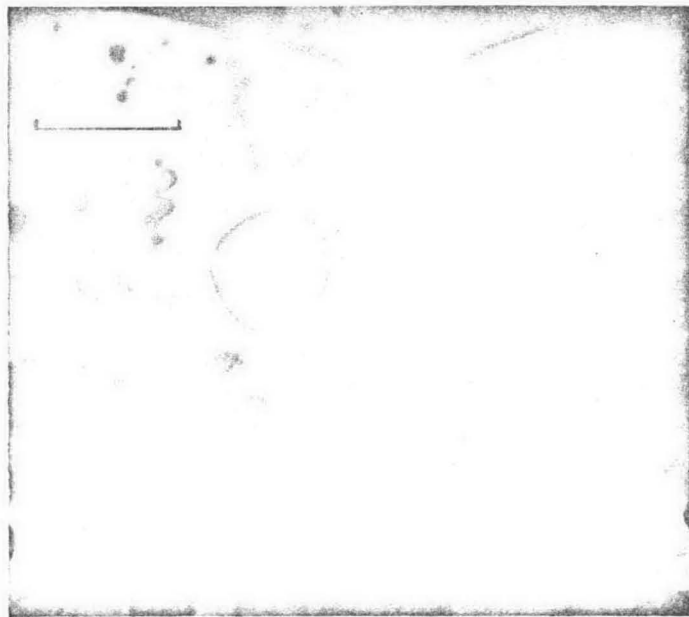
The structure of doped PM tungsten recrystallized at 2200°C for 30 min is illustrated in fig. 1 (a). This particular annealing temperature was selected because it results in a sub-structure which contains a low density of dislocations with a void-matrix interface almost free from dislocations. The rows of circular areas, which lie along the axis of the wire, have been identified by diffraction contrast analysis as internal voids (Das and Radcliffe 1968 a). The size of the voids ranges between 100 Å and 1000 Å. The sub-structure of the tungsten-thoria alloy recrystallized at 2200°C for 30 min (fig. 1 b) exhibits isolated rounded particles of thoria ranging in size from 0.1 to approximately 1 micron and free from dislocations. However, sub-boundaries consisting of hexagonal networks of dislocations are observed in the tungsten matrix. In the case of the tungsten-HfC alloy, the hafnium carbide particles were also free from dislocations. The shapes of the hafnium carbide particles are more angular (fig. 1 c) and their size range smaller than for the ThO₂ particles.

The sub-structures of the matrix adjacent to the elastic discontinuities in the as-recrystallized condition and after pressurization were carefully compared under various diffraction conditions. Up to pressures as high as 25 kilobars, no evidence of dislocations or other defects due to pressurization was found in the vicinity of voids or particles of thoria or hafnium carbide. These observations are in keeping with the calculations made in § 2 in that at 25 kilobars (see table 2), the maximum values of shear stress developed for the cases of void, thoria and hafnium carbide particles are $G/80$, $G/360$, $G/520$, respectively, which are substantially lower than the stress for nucleating dislocations. However, on pressurizing the thoria and hafnium carbide alloys at 40 kilobars, new dislocations were developed, as illustrated in fig. 2. Around the larger thoria particles (fig. 2 a), complex dislocation arrays appear which are analogous to those observed (Radcliffe and Warlimont 1964) at iron carbide particles in an alpha-iron matrix on pressurization above some 5 kilobars. The areas adjacent to the smaller particles appeared unaffected by the pressure treatment. No well-developed prismatic dislocation loops were found. In contrast, in the case of HfC particles (fig. 2 b), well-developed rows of dislocation loops characteristic of prismatic punching were observed. The fact that these differences in the type of dislocation array persist for thoria and hafnium carbide particles of similar sizes indicates that the different compressibilities of the two compounds (both of cubic structure) play a significant role in determining the nature of the array formed.

Fig. 1

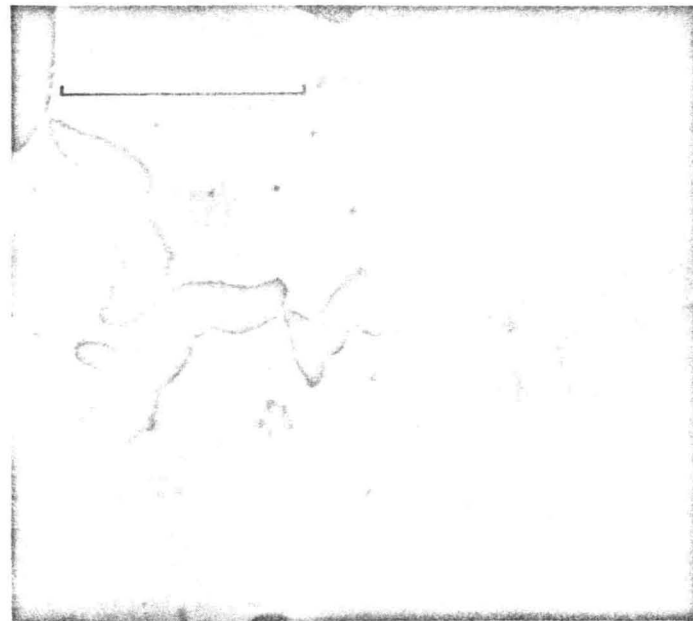


(a)



(b)

Fig. 1 (continued)

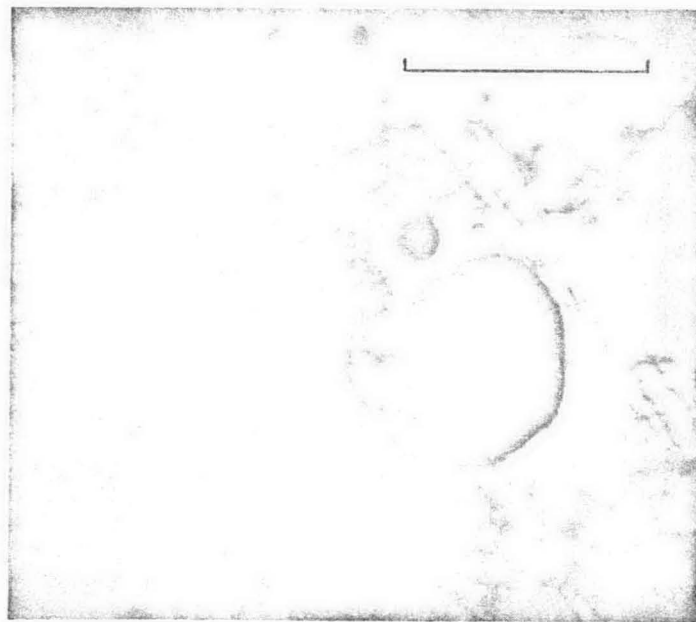


(c)

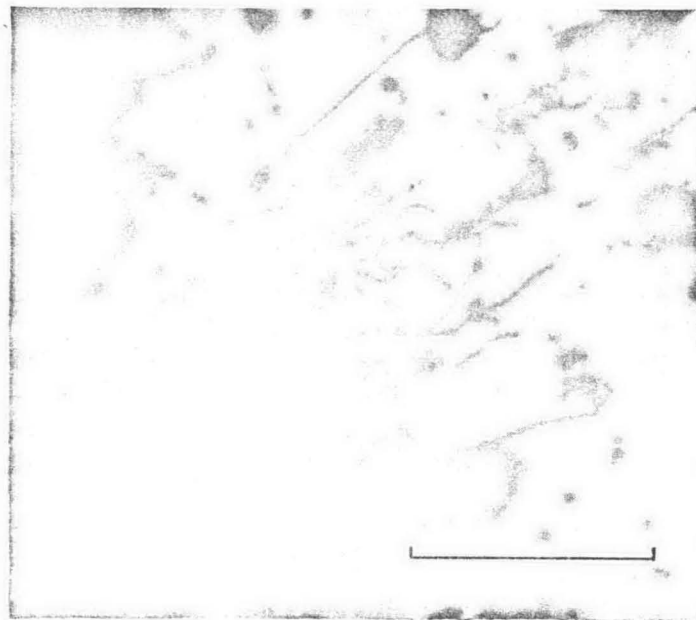
Thin foil electron micrographs illustrating structures of: (a) doped PM tungsten recrystallized at 2200°C (longitudinal wire section); (b) PM tungsten-0.9 vol. % ThO₂ alloy recrystallized at 2200°C (transverse section); (c) tungsten-1.4 vol. % HfC alloy after precipitation treatment. The scale markers designate 1 micron.

It must be noted that since the particles in the tungsten are larger than the foil thickness, unlike the case referred to earlier of carbide particles in iron (Radeliffe and Warlimont 1964), the association of the pressure-induced dislocations with any particular particle is not unequivocal. The iron did contain occasional impurity particles (iron oxide) which were also larger than the foil thickness, but their isolation enabled them to be identified as the source of associated dislocation arrays induced by pressurization, whereas the closer spacing of the particles in the tungsten makes such unique identification difficult. However, the possibility of such dislocations arising from mishandling of the foils can be rejected because of the characteristic brittle behaviour of tungsten at room temperature and, furthermore, the nature of the arrays is very different from those formed when tungsten is plastically strained at room temperature, as shown recently from tensile tests in which fracture is suppressed by increasing the environmental pressure (Das and Radeliffe 1968 c).

Fig. 2



(a)



(b)

Pressure-induced dislocations sub-structures observed in the vicinity of second-phase particles in tungsten after pressurization to 40 kilobars: (a) 0.9 vol. % ThO_2 alloy; (b) 1.4 vol. % HfC alloy.

4.1.
T
tung
valu
tho
stil
vie
obs
str
pre
rec
ex
He
co
sit

(F
su
le
ir
e
t
f
s
g
l
e
i
:

4.1.1. Dislocation nucleation

The observations of the pressure-induced dislocations at 40 kilobars in tungsten at the particle/matrix interface regions is surprising in that the values of maximum shear stress τ_{\max} attainable in both the cases of thoria and hafnium carbide particles, $G/225$ and $G/325$, respectively, are still much below the nucleation stress for dislocation generation. In view of the discrepancy between the stress at which dislocations are observed experimentally and the theoretically predicted magnitude of the stress to nucleate dislocations (Cottrell 1964), the assumption made in the present calculations that the particle is spherical with a smooth surface requires further examination. Real particles would be expected to exhibit sharp steps at their interfaces and are seldom truly spherical. Hence, the stresses in the region containing a sharp step or angularity could be increased in such a way that these areas would become preferred sites for dislocation nucleation.

In the case of a small indenter (10^{-4} cm diameter) on a free surface (Friedel 1963)—e.g. silicon carbide particles dropped onto a crystal surface—a contact pressure of $10^{-3} G$ is sufficient to punch in dislocation loops. This observation can be explained only if it is assumed that the indenter possesses atomistically sharp steps. The appropriate stress concentration of $2(D/2b)^{1/2}$ (where D is the particle diameter and b is the Burgers vector of the dislocation) corresponds to a stress concentration factor of about 100 for a 1 micron particle and the stress at the edge of such an indenter becomes of the order of $10^{-1} G$, as required for dislocation generation. From the calculated magnitude of the shear-stresses induced by differential compression, as shown in table 2, it is apparent that the experimentally observed dislocations could be explained if irregularities in the shapes of the particles or sharp steps on their surfaces acted as stress raisers.

The generation of dislocations on pressurization could also be influenced by the existence of residual stresses around the interface of the inclusion and matrix, such as frequently arise from differential thermal contraction effects during cooling from the annealing temperature. The recent literature contains a number of observations (Leslie 1961, Patel 1962, Kayano 1967 a, b) of particles under applied shear stress acting as dislocation sources; particularly good examples of punched-in dislocations are those formed around FeO particles in iron deformed 2% in tension reported by Kayano, who concluded that residual stresses around the inclusion resulting from cooling must assist dislocation generation during subsequent tensile deformation. Thus, in systems in which thermal stresses of appropriate sign are induced, the existence of residual stresses should similarly assist the generation of dislocations during pressurization and consequently influence the magnitude of the critical pressure observed.

The development of pressure-induced dislocations around thoria or hafnium carbide particles in tungsten (as also for helium bubbles in copper, which will be discussed in detail later) is noticeably dependent on the size

of the inclusion. However, the calculation in § 2 indicates that the value of the maximum shear stress attainable at the interface is independent of the size of the elastic discontinuity. This apparent paradox can be resolved if the details of the conditions necessary for the propagation of dislocations from the particle/matrix interface are taken into account. On this basis, a segment of dislocation is generated at the interface of a particle, independent of its size, when the pressure-induced shear stress reaches an appropriate value. However, the achievement of a full prismatic loop which can move away from the particle is strongly size dependent, as shown by the following argument.

It is apparent from fig. 3 (a) that a dislocation (at L) of radius of curvature $a/\sqrt{2}$, where a is the radius of the discontinuity, nucleated on the circle of maximum shear stress marked II can glide under the action of shear stress parallel to its Burgers vector and the axis of the indicated glide cylinder (i.e. the shear stress circle marked I). The resulting development of a full prismatic loop thus occurs in accordance with the 'punching' mechanism suggested originally by Seitz (1950) and modified for the thermal stress case by Jones and Mitchell (1958). The shear forces developed as a result of differential compression must support the line tension, F , of the dislocation, which can be written as:

$$F = \frac{Gb^2}{4\pi(1-\nu)} \left\{ \ln \frac{R}{b} + 1 \right\}, \quad \dots \dots \dots (6)$$

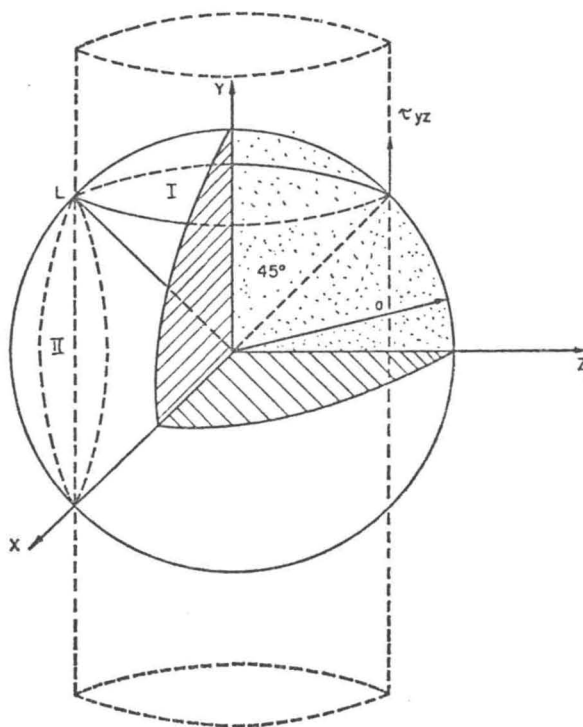
where R is the radius of the loop and b is the Burgers vector. For small loops of the order of 500 Å (i.e. 200 b), F can be approximated as $Gb^2/2R$ and equated† with the work done by τ_{\max} at L:

$$\tau_{\max} b = \frac{Gb^2}{2R} \cdot \dots \dots \dots (7)$$

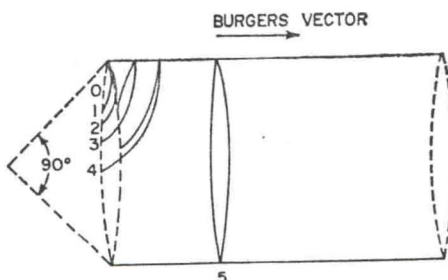
Equation (7) demonstrates that a pressure giving a shear stress which is sufficient to achieve the complete loop stage for a discontinuity of given diameter will be too small to reach this stage for a particle of smaller diameter. However, despite the qualitative agreement with observation, numerical calculations for the various tungsten cases based on this simple approach give critical sizes of discontinuity which are approximately one order of magnitude smaller than those at which dislocations were observed experimentally. In the case of copper, to be discussed later, closer quantitative agreement was obtained.

† Recently and independently, a similar argument has been used for the case of the generation of glide dislocation loops by thermal stresses induced by quenching (Gulden and Nix 1968) to compute the critical particle size necessary to form the initial complete dislocation loop.

Fig. 3



(a)



(b)

(a) Spherical 'particle' of radius a in a matrix subjected to external hydrostatic pressure. The intersection of the 90° cone with the surface of the sphere corresponds to a circle of maximum induced shear stress and defines the glide cylinder, shown by the dashed lines, for the induced dislocation loops. (b) Schematic illustration of the stages of formation of a full prismatic loop at a spherical 'particle' under the action of pressure-induced shear stresses. At stage 5, the loop is capable of gliding along the cylinder, which has its axis parallel to the Burgers vector.

that the value is independent of the radius of the particle. This paradox can be explained by the propagation of dislocations into account. At the interface of a particle, the induced shear stress is of the order of a full dislocation of a strongly size

of radius of the particle, nucleated on the surface under the action of the indicated shear stress. The resulting dislocation balance with the applied stress and modified dislocation density. The shear stress support the

(6)

For small particles, the induced shear stress is estimated as $Gb^2/2R$

(7)

stress which is of the order of the yield strength of given material. For a particle of smaller radius, the induced shear stress, based on this model, are approximately of the order of the yield strength of the matrix. This dislocation density to be discussed

is used for the estimation of the stresses induced by the dislocations of the size necessary

4.1.2. Dislocation multiplication

Although the mechanism of dislocation generation due to stress concentrations at the surface irregularities of the particles appears feasible, the possibility of the induced stress at the particles causing multiplication of pre-existing interface dislocations cannot be overlooked. Thus, such a dislocation could operate as a Frank-Read source when the induced shear stress exceeds a critical value and gives rise to prismatically punched dislocation loops or dislocation tangles. The stress to operate a source of one micron (i.e. the full particle diameter) would be as low as $G/3650$ in tungsten. Experimental measurements (Garfinkle 1966) of proportional limits for high-purity tungsten single crystals give flow stresses of a similar order of magnitude (5000 p.s.i.). The computed pressure to develop such relatively low stresses at the interface of elastic discontinuities is less than 10 kilobars.

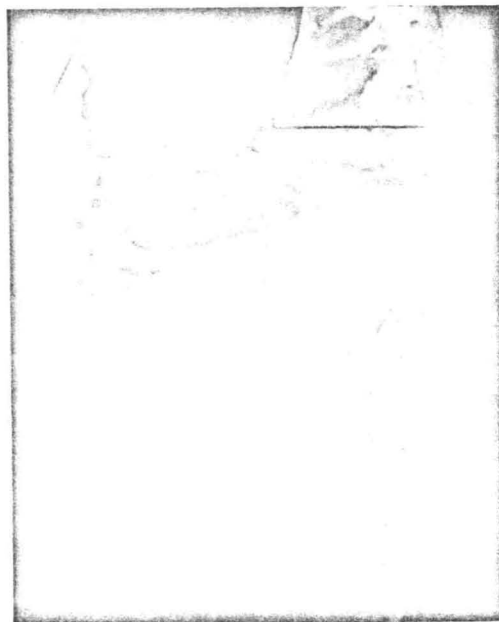
For the voids in the PM tungsten matrix, the value of the maximum shear stress computed for 25 kilobars from the mathematical model is $G/80$, which is much higher than the value estimated above for dislocation multiplication. However, no new dislocations were observed experimentally around voids after pressurization up to 25 kilobars. In the case of thoria and hafnium carbide particles, where the computed maximum values of the shear stress are $G/360$ and $G/520$, respectively, at 25 kilobars, again no dislocation generation was observed after pressure cycling. From these arguments and observations it is deduced that pressure-induced dislocations in the tungsten are unlikely to be due to multiplication of pre-existing dislocations and that stress concentrations at the matrix-particle interface appear necessary to explain their formation.

4.2. Copper Containing Helium-filled Cavities

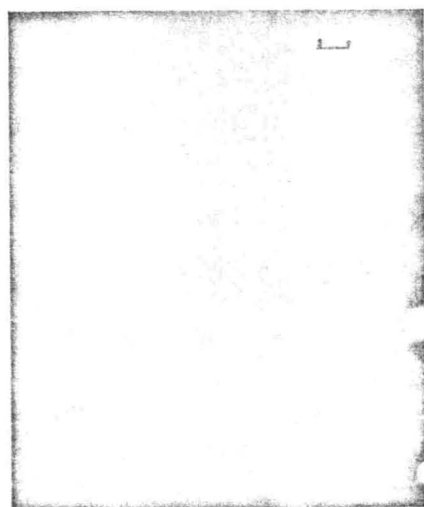
The high energy (43 mev) α -particles penetrated the copper to a depth of some 0.01 in. from the irradiated surface and came to rest in a narrow layer at that depth. The width of the layer or band of bubbles of He precipitated in this region on annealing was 0.006 in. Previous electron microscopy studies of helium precipitation in irradiated copper (Barnes *et al.* 1958, Barnes and Mazey 1960, Ghosh *et al.* 1960) have been restricted, because of the difficulties of specimen preparation, to thin foils prepared parallel to the plane of the He-rich band. The high precision microjet thinning method developed for the present study has permitted the observation of the structural features across the entire width of the band.

As illustrated in fig. 4, the structure of the band in the irradiated and annealed copper consists of large spherical bubbles (1000 Å average diameter) in the outermost regions at both sides of the band and a dense population of very small bubbles (60–70 Å in diameter) in the interior of the band. The bubbles are generally free from dislocations, except for occasional interconnecting dislocations. In contrast, after pressurization to 25 kilobars, pressure-induced dislocations are visible in the matrix at

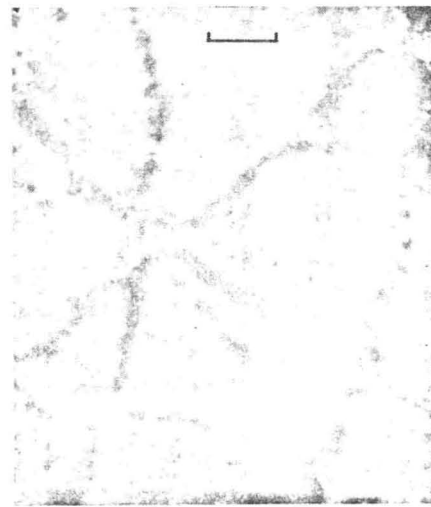
Fig. 4



(a)



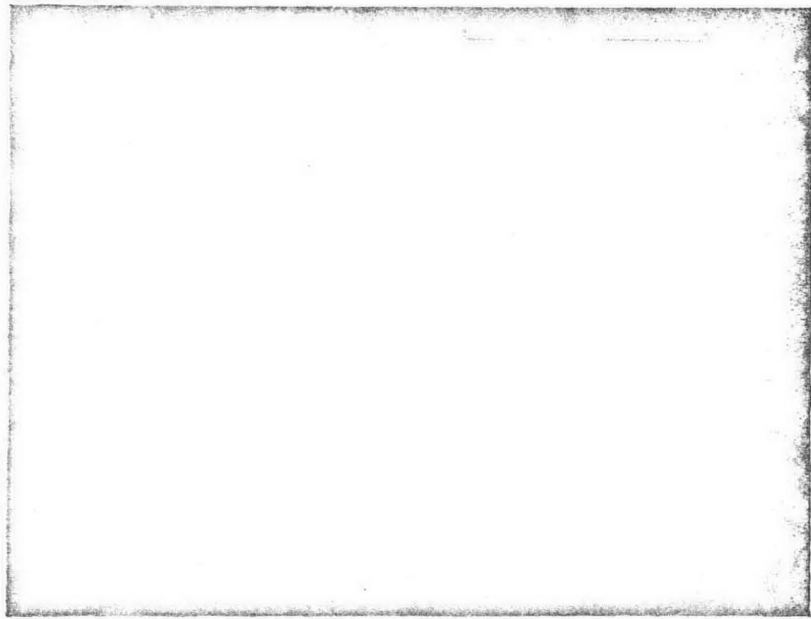
(b)



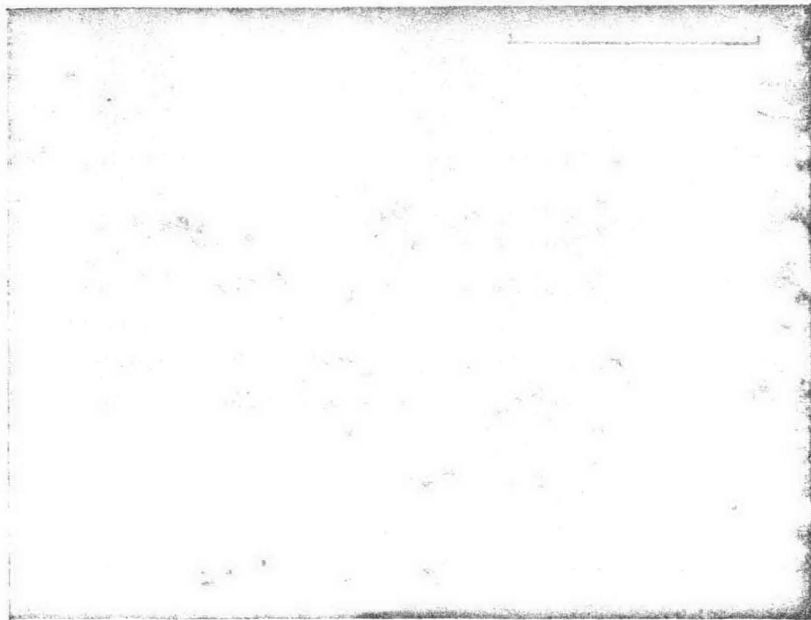
(c)

Distribution of helium-filled bubbles in irradiated and annealed copper: (a) dark-field micrograph illustrating the changes in bubble structure across the full width of the helium-rich band; (b) large bubbles (average diameter 1000 Å) formed in the outermost regions of the band; (c) high density of small bubbles (average diameter 60 Å) formed within the band. The markers indicate 10 microns in (a) and 0.1 microns in (b) and (c).

Fig. 5

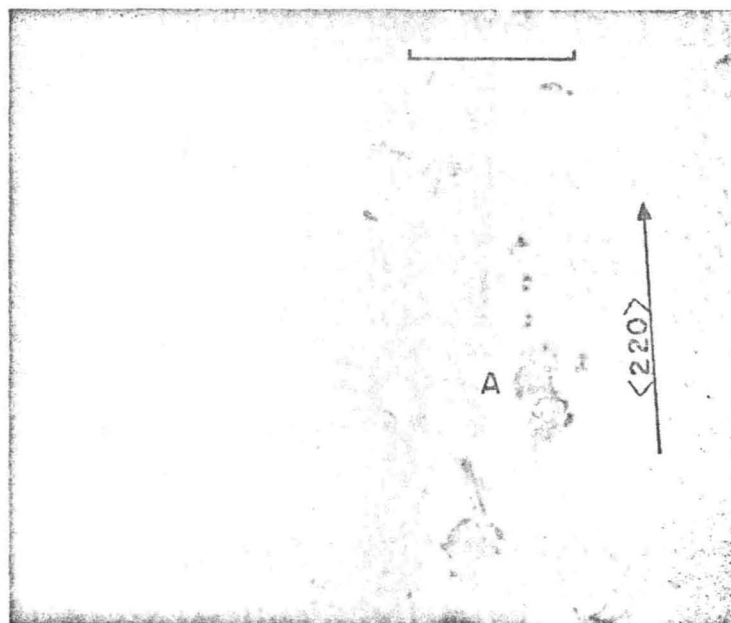


(a)



(b)

Fig. 5 (continued)



(c)

Dislocations observed at helium-filled bubbles in copper following subjection to an external hydrostatic pressure of 25 kilobars: (a) example of influence of bubble size on development of pressure-induced dislocations; (b) dense dislocation tangles observed at largest bubbles, together with examples of changes in the shape of the originally spherical bubbles; (c) simple array of prismatically punched loops developing along $\langle 220 \rangle$ direction from a helium bubble (marked A). The markers indicate 1 micron.

many of the bubbles (fig. 5). Around the larger (500–1500 Å) bubbles, dislocations are seen as a dense 'woolly' tangle somewhat similar to that reported for Fe_3C particles in iron (Radcliffe and Warlimont 1964). Some of the bubbles which have dislocations associated with them no longer have the spherical shapes seen in the annealed structure. Figure 5 (c) illustrates well-developed prismatic dislocation loops which develop along $\langle 220 \rangle$ directions. In contrast to these features associated with the large bubbles, the smaller bubbles situated in the interior of the band appear unaffected by the pressurization. The minimum size of bubble that was observed to be effective in generating dislocations is 500 Å. In a few cases (see fig. 5 a, b) bubbles of an average size less than 500 Å also appear non-spherical in shape, but without having dislocations visible around them even when examined carefully over a range of diffraction contrast conditions.

The above observations of dislocation generation under pressure are in keeping with the conditions calculated earlier (see table 2). The computed value of the maximum shear stress generated at the bubble-matrix interface at 25 kilobars is $G/27$, which is larger than the estimated critical stress for the nucleation of dislocations in copper. Moreover, the facts that the smaller bubbles (60 Å in diameter) appear insensitive to pressurization and the minimum size of the bubbles required for dislocation generation is about 500 Å are in keeping with the arguments presented earlier as to the influence of size. It must be noted that the critical pressure required to form these new dislocations was not determined experimentally, since pressurization was carried out at 25 kilobars only—a pressure selected because the value of the maximum shear stress calculated for this pressure approaches the nucleation stress for dislocations. However, although additional experiments at lower pressures would be needed to distinguish unequivocally between the operation of nucleation or multiplication mechanisms for the development of the pressure-induced dislocations, the latter mechanism is considered unlikely in view of the fact that dislocations associated with the bubbles were observed only rarely prior to pressurization.

While the present results appear to be first direct observations of dislocations induced around gas bubbles in a metal matrix by the application of external hydrostatic pressure, indirect experimental evidence for this type of localized plastic deformation has been reported by Miles and Gibbs (1964) who noted permanent changes in the amplitude-dependent internal friction of air-melted polycrystalline aluminium after pressurization to 6 kilobars. The changes could be eliminated by annealing and did not occur in zone-refined aluminium. However, after re-melting in hydrogen the effect could be induced in the latter material also. It was deduced from these observations that the observed irreversible effects were due to the relaxation (Snoeck damping) of dislocations which had been formed at hydrogen-filled internal cavities when the specimens were subjected to high external pressure—i.e. an hypothesis in keeping with the experimental observations made here for copper. Additional evidence for pressure-induced plastic deformation at internal cavities was reported recently by Norris (1964) for lead iodide crystals (containing bubbles filled with iodine vapour) pressurized to 26 kilobars. Limited electron microscopy observations showed changes in contrast following pressurization which were interpreted as due to deformation of the gas bubbles and the formation of pressure-induced dislocations.

Direct observations of rows of prismatic dislocation loops in magnesium analogous to those developed here in copper on external pressurization have been reported by Lally and Partridge (1966) for the inverse case of internal pressurization of hydrogen-filled cavities. The loops were observed in experiments at atmospheric pressure in which magnesium was heated and quenched in such a manner as to absorb hydrogen and then precipitate it in the form of small bubbles of high internal pressure.

Using an extension of Eshelby's (1957) solution for the shear stresses around a misfitting inclusion having the same elastic constants as the matrix, with inclusion and matrix being elastically isotropic, Lally and Partridge showed that shear stresses will develop in the matrix adjacent to the hydrogen-filled cavity. Comparison of their eqn. (1) for shear stress with that given here for the same problem indicates that the two approaches apparently agree only for the condition that $\nu = \frac{1}{2}$. However, a recalculation based on the Eshelby model used by Lally and Partridge has indicated an error in their calculation and confirmed the correctness of the form of equation developed in the present work. Nevertheless, the hypothesis that the dislocation loops in magnesium are generated as the result of shear stress arising from the internal pressure remains valid and provides further support for the analysis presented in the present paper concerning similar phenomena developed by external pressure.

The stress field which arises around an internal discontinuity (cavity or inclusion) as a result of differential compression on pressure application is analogous to that which is developed due to differential thermal contraction during cooling. Accordingly, it might be expected that the nature of such pressure-induced dislocations would be similar to that of those induced thermally. Although a complete diffraction contrast analysis of pressure-induced dislocations has not yet been reported and has not proved possible in the present study, both the mechanism of loop formation (Jones and Mitchell 1958) and the nature of the loops (Lawley and Meakin 1964) have been examined for the thermal case. For such loops at spherical glass particles in silver chloride, Jones and Mitchell showed the successive stages of formation (as illustrated in fig. 3 *b*) to be nucleation of a dislocation segment in the region of maximum shear, followed by glide of the edge component away from the sphere along the surface of the glide cylinder and of the two screw components in opposite directions around the cylinder until they meet to form a full prismatic loop. Using transmission microscopy, Lawley and Meakin showed that loops formed in a similar manner at carbide particles in molybdenum were interstitial in nature. The thermal and pressure cases are completely analogous when the discontinuity is a particle and the generation of interstitial loops would act in both cases to reduce the locally induced stresses by transporting material away from the particle-matrix interface. However, for an internal cavity (depending on the relative magnitudes of the internal and external pressures) the appropriate relaxation could require transport of vacancies away from the cavity, i.e. the formation of vacancy loops. The shape changes observed here for the cavities in copper (see fig. 5 *b*) are in keeping with such a mechanism.

§ 5. SUMMARY AND CONCLUSIONS

The stress fields developed at internal cavities, and rigid and elastic inclusions in an isotropic solid subjected to external hydrostatic pressure have been computed and compared with experimental observations of

pressure-induced development of dislocations at elastic discontinuities in tungsten and copper. The principal results and conclusions are:

(1) In tungsten containing second-phase particles of thoria or hafnium carbide, the formation of pressure-induced dislocations at particles occurs for applied pressures which are lower than those predicted from the simple mathematical model. It is shown that additional stress concentrations from irregularities on the particle surfaces, possibly assisted by residual thermally-induced stresses, could account for these differences.

(2) The magnitude of the applied pressure found to be necessary to develop dislocations at the particles precludes multiplication of pre-existing dislocations as the relevant mechanism.

(3) For copper containing helium-filled internal cavities, the magnitude of the externally applied pressure required to develop dislocations at the cavities is in reasonable agreement with that computed from the model.

(4) The observed development of pressure-induced dislocations at cavities in copper supports earlier interpretations of pressure-induced permanent changes in the internal friction characteristics of aluminium as being due to localized plastic-deformation at cavities.

(5) For both tungsten and copper, the development of pressure-induced dislocations is observed to depend strongly on the size of the discontinuity. This result is shown to be in reasonable agreement—particularly for the case of cavities in copper—with computation of the size dependence of the energy necessary to nucleate a stable dislocation loop at a discontinuity.

ACKNOWLEDGMENTS

The authors wish to express their thanks to Dr. A. D. Rossin of the Argonne National Laboratory, U.S. Atomic Energy Commission for assistance in carrying out the cyclotron irradiation experiment and to their colleagues in the High Pressure Group and Dr. R. A. Clark, Department of Mathematics, for helpful discussions.

The use of the facilities in the Department of Metallurgy and Materials Science and in the Center for the Study of Materials is appreciated and the support of the National Aeronautics and Space Administration is gratefully acknowledged.

REFERENCES

- ANDREWS, C. W., and RADCLIFFE, S. V., 1967, *Acta metall.*, **15**, 623.
BARNES, R. S., and MAZEY, D. J., 1960, *Phil. Mag.*, **5**, 1247.
BARNES, R. S., REDDING, G. B., and COTTRELL, A. H., 1958, *Phil. Mag.*, **3**, 97.
BULLEN, F. P., HENDERSON, F., HUTCHISON, M. M., and WAIN, H. L., 1964, *Phil. Mag.*, **9**, 285.
COTTRELL, A. H., 1964 a, *Theory of Crystal Dislocations* (New York: Gordon & Breach); 1964 b, *The Mechanical Properties of Matter* (New York: John Wiley).

- DAS, G., and RADCLIFFE, S. V., 1968 a, *Trans. Am. Inst. Min. Metall. Engrs.*, **242**, 2029; 1968 b, *Electron Microscopy* (Proc. Fourth European Conf. Rome, Sept. 1968), Vol. 1 (Rome: Tip. Polig. Vaticana), p. 259; 1968 c, *J. Japan Inst. Metals*, **9**, 334.
- EDWARDS, R. H., 1951, *J. appl. Mech.*, **18**, 19.
- ESHELBY, J. D., 1957, *Proc. R. Soc. A*, **241**, 376.
- FRIEDEL, J., 1963, *Electron Microscopy and the Strength of Crystals*, edited by G. Thomas and J. Washburn (New York: Interscience), p. 605.
- GARFINKLE, M., 1966, *Trans. Am. Inst. Min. Metall. Engrs.*, **236**, 1373.
- GARROD, R. F., and WAIN, H. L., 1965, *J. less-common Metals*, **9**, 81.
- GHOSH, T. K., BEEVERS, C. J., and BARNES, R. S., 1960, *J. Inst. Metals*, **89**, 125.
- GOODIER, J. N., 1933, *J. Am. Soc. Mech. Engrs.*, **55**, APM-55-7-39.
- GULDEN, M. G., and NIX, W. D., 1968, *Phil. Mag.*, **18**, 217.
- HAHN, G. T., and ROSENFELD, A. R., 1966, (Battelle Mem. Inst. Rept), Tech. Rept. AFML-TR-65-409. U.S. Air Force Material Laboratory, Dayton, Ohio.
- JONES, D. A., and MITCHELL, J. W., 1958, *Phil. Mag.*, **3**, 1.
- KAYANO, H., 1967 a, *J. Japan Inst. Metals*, **31**, 310; 1967 b, *Ibid.*, **31**, 316.
- LALLY, J. S., and PARTRIDGE, P. G., 1966, *Phil. Mag.*, **13**, 9.
- LAWLEY, A., and MEAKIN, J. D., 1964, *Phil. Mag.*, **10**, 737.
- LAMÉ, G., 1852, *Léçons sur la théorie . . . de l'élasticité* (Paris).
- LESLIE, W. C., 1961, *Acta metall.*, **9**, 1004.
- MILES, M. H., and GIBBS, P., 1964, *J. appl. Phys.*, **35**, 1941.
- NABARRO, F. R. N., 1940, *Proc. R. Soc. A*, **175**, 519.
- NORRIS, D. I. R., 1964, *Electron Microscopy*, Vol. A (Proc. Third European Conf. Prague, Sept. 1964) (Prague: Czech. Acad. Sci.), p. 319.
- PATEL, J. R., 1962, *J. appl. Phys.*, **33**, 2223.
- RADCLIFFE, S. V., 1964, *Irreversible Effects Produced by High Pressure Treatment* (International Conference on Materials, Philadelphia, Feb. 1964), (Philadelphia: Am. Soc. Test. Materials), p. 141; 1969, Chapter XI, *Mechanical Behaviour of Materials Under Pressure*, edited by H. Ll. D. Pugh (Amsterdam: Elsevier Publishing Co.), in press.
- RADCLIFFE, S. V., and WARLIMONT, H., 1964, *Phys. Stat. Sol.*, **7**, 67.
- SEITZ, F., 1950, *Phys. Rev.*, **79**, 723.
- SHAFFER, P. T. B., 1964, *High Temperature Materials* (New York: Plenum Press).
- SOKOLNIKOFF, I., 1956, *Mathematical Theory of Elasticity* (New York: McGraw Hill Book Company Inc.).
- TANNER, L. E., and RADCLIFFE, S. V., 1962, *Acta metall.*, **10**, 1161.

discontinuities
ions are:
ia or hafnium
articles occurs
om the simple
concentrations
d by residual
nces.

necessary to
ation of pre-

s, the magni-
p dislocations
ted from the

dislocations at
ssure-induced
of aluminium

of pressure-
e size of the
agreement—
tation of the
le dislocation

Rossin of the
mission for
ment and to
lark, Depart-

and Materials
preciated and
inistration is

323.

l. Mag., **3**, 97.
, H. L., 1964,

rk: Gordon &
(New York: